The Astrophysical Journal, 680:926–938, 2008 June 20


# ON THE NATURE OF SEYFERT GALAXIES WITH HIGH [O III] λ5007 BLUESHIFTS

S. Komossa
Max-Planck-Institut für extraterrestrische Physik, Giessenbachstrasse 1, 85748 Garching, Germany; skomossa@mpe.mpg.de

D. Xu
National Astronomical Observatories, Chinese Academy of Science, A20 Datun Road, Chaoyang District, Beijing 100012, China

H. Zhou
Max-Planck-Institut für extraterrestrische Physik, Giessenbachstrasse 1, 85748 Garching, Germany

T. Storchi-Bergmann
Instituto de Fisica, UFRGS, Campus do Vale, CP 15051, Porto Alegre 91501-970, RS, Brazil

AND

L. Binette
Département de Physique, de Génie Physique et d'Optique, Université Laval, Québec, QC G1K 7P4, Canada; and Instituto de Astronomia, UNAM, Ap. 70-264, 04510 México, DF, México
*Received 2007 December 12; accepted 2008 February 28*

## ABSTRACT

We have studied the properties of Seyfert galaxies with high [O III] λ5007 blueshifts ("blue outliers"), originally identified because of their strong deviation from the $M_{BH}$-$\sigma$ relation of normal, narrow-line Seyfert 1 (NLS1) and broad-line Seyfert 1 (BLS1) galaxies. These blue outliers turn out to be important test beds for models of the narrow-line region (NLR), for mechanisms of driving large-scale outflows, for links between NLS1 galaxies and radio galaxies, and for orientation-dependent NLS1 models. We report the detection of a strong correlation of line blueshift with ionization potential in each galaxy, including the measurement of coronal lines with radial velocities up to 500–1000 km s$^{-1}$, and we confirm a strong correlation between [O III] blueshift and line width. All [O III] blue outliers have narrow widths of their broad Balmer lines and high Eddington ratios. While the presence of nonshifted low-ionization lines signifies the presence of a classical outer quiescent NLR in blue outliers, we also report the absence of any second, nonblueshifted [O III] component from a classical inner NLR. These results place tight constraints on NLR models. We favor a scenario in which the NLR clouds are entrained in a decelerating wind, which explains the strong stratification and the absence of a zero-blueshift inner NLR of blue outliers. The origin of the wind remains speculative at this time (collimated radio plasma, thermal winds, or radiatively accelerated clouds). It is perhaps linked to the high Eddington ratios of blue outliers. Similar, less powerful winds could be present in all Seyfert galaxies, but would generally only affect the coronal line region (CLR), or level off even before reaching the CLR. Similarities between blue outliers in NLS1 galaxies and (compact) radio sources are briefly discussed.

*Subject headings:* galaxies: active — galaxies: evolution — galaxies: individual (SBS 0919+515, SDSS J115533.50+010730.4, RX J01354−0043, NGC 450-86, SDSS J032606.75+011429.9, IRAS 11598−0112, SDSS J171828.99+573422.3, PG 1244+026, RX J09132+3658) — galaxies: Seyfert — quasars: emission lines

*Online material:* color figures

## 1. INTRODUCTION

The concept of feedback due to outflows is a potential key ingredient in understanding the coevolution of galaxies and black holes (Silk & Rees 1998; Fabian 1999; Wyithe & Loeb 2003). Recent analytic estimates and simulations demonstrate the importance of feedback from winds/outflows; for instance, in cosmic downsizing (Scannapieco et al. 2005), in fixing the $M_{BH}$-$\sigma$ relation (di Matteo et al. 2005), and in determining galaxy colors (Springel et al. 2005) by regulating star formation in the host galaxy. Powerful gaseous outflows in active galactic nuclei (AGNs) deposit mass, energy, and metals in the interstellar medium of the galaxy and the intergalactic medium or intracluster medium (Colbert et al. 1996; Churazov et al. 2001; Moll et al. 2007). AGN winds also play a potentially important role in unified models of AGNs (Elvis 2000, 2006).

Observational evidence for outflows in AGNs exists on various scales and in all wave bands from the radio (Morganti et al. 2005; Gallimore et al. 2006) to the IR (Rodriguez-Ardila et al. 2006), optical (Das et al. 2005), UV (Sulentic et al. 2007; Rodriguez Hidalgo et al. 2007; Crenshaw & Kraemer 2007), and X-ray (Chelouche & Netzer 2005; Krongold et al. 2007) bands; see Veilleux et al. (2005) for a review. There are several lines of evidence that outflows are particularly strong in narrow-line Seyfert 1 (NLS1) galaxies. NLS1 galaxies are a subclass of AGNs with extreme emission-line and continuum properties which appear to be in part driven by their high Eddington ratios, low black hole masses, and other parameters (e.g., Osterbrock & Pogge 1985; Boroson 2002; Grupe 2004; see Komossa 2008 for a review). The high Eddington ratios likely lead to strong, radiation-pressure-driven outflows.

As a class of objects with low black hole masses, high accretion rates, and strong winds, the location of NLS1 galaxies on the $M_{BH}$-$\sigma$ plane is of special interest (Mathur et al. 2001; see our § 4.1). Komossa & Xu (2007, hereafter KX07) have shown that NLS1 galaxies follow the same $M_{BH}$-$\sigma$ relation as normal and

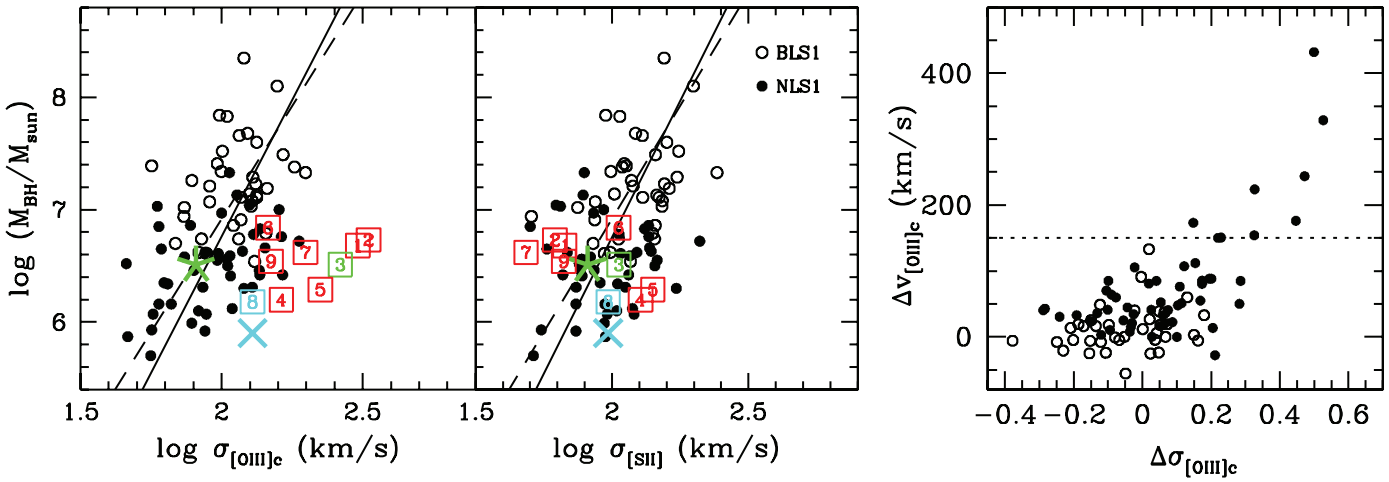


FIG. 1.—Location of blue outliers (*open squares*) on the $M_{\rm BH}$-$\sigma$ plane in comparison to the full NLS1 (*filled circles*) and BLS1 (*open circles*) sample (KX07). *Left*: The leftmost panel is based on $\sigma$ measurements from the narrow core of [O III] $\lambda$5007 (asymmetric blue wings were removed). Blue outliers in [O III] (with radial velocities larger than 150 km s$^{-1}$) are marked with an open square. Object names are coded by number (1, SBS 0919+515; 2, SDSS J11555+0107; 3, RX J01354−0043; 4, NGC 450-86; 5, SDSS J03261+0114; 6, IRAS 11598−0112; 7, SDSS J17184+5734; 8, PG 1244+026; 9, RX J09132+3658). The second panel shows the same relation based on [S II]. NLS1 and BLS1 galaxies follow the same $M_{\rm BH}$-$\sigma_{\rm [SII]}$ relation. The dashed and solid lines represent the $M_{\rm BH}$-$\sigma_*$ relation of nonactive galaxies of Tremaine et al. (2002) and Ferrarese & Ford (2005), respectively. Two objects with independent BH mass (PG 1244+026) and stellar velocity dispersion (RX J01354−0043) estimates are marked with special symbols (*blue cross*: PG 1244+026; *green asterisk*: RX J01354−0043). *Right*: Deviation $\Delta\sigma$ of NLS1 and BLS1 galaxies from the $M_{\rm BH}$-$\sigma_*$ relation of Ferrarese & Ford (2005) in dependence of [O III] radial velocity, $\Delta v$, measured with respect to [S II].

broad-line Seyfert 1 (BLS1) galaxies, if the width of the [S II] $\lambda\lambda$6716,6731 emission lines is used as a surrogate for stellar velocity dispersion. The width of [O III] $\lambda$5007 (after removal of asymmetric blue wings) is still a good proxy for stellar velocity dispersion in BLS1 and NLS1 galaxies, with one important exception. A subset of NLS1 galaxies deviates systematically from the $M_{\rm BH}$-$\sigma$ relation, and all of these are characterized by high [O III] *blueshifts*. At the same time, the [S II]–based measurements of the velocity dispersion of the same objects still place them *on* the $M_{\rm BH}$-$\sigma$ relation (Fig. 1). Therefore, the [O III] lines of these particular galaxies were not suitable to estimate $\sigma$. However, the independent question is raised as to which mechanism drives these [O III] line blueshifts, and what we can learn from them regarding the nature of these systems and perhaps the evolutionary state of NLS1 galaxies. That is the topic of this study.

A measurable difference in blueshifts and widths of different NLR emission lines has been recognized early (review by Osterbrock 1991). The phenomenon of strong [O III] blueshifts exceeding 100 to several hundred km s$^{-1}$ (so-called blue outliers) is more rare. It has been detected early in individual objects (Phillips 1976) but has only been studied systematically recently (Zamanov et al. 2002; Marziani et al. 2003; Aoki et al. 2005; Boroson 2005; Bian et al. 2005). These studies have shown that blue outliers have high Eddington ratios and small Balmer line widths [all of them with FWHM(H$\beta$) $< 4000$ km s$^{-1}$, and most of them with FWHM(H$\beta$) $< 2000$ km s$^{-1}$; Marziani et al. 2003]. It has remained uncertain whether there is (Bian et al. 2005) or is not (Aoki et al. 2005) a direct correlation between [O III] blueshift and Eddington ratio. Common to most studies is the presence of a strong correlation between [O III] blueshift and [O III] line width. This correlation is also known among iron coronal lines of BLS1 galaxies (Penston et al. 1984; Erkens et al. 1997). The reason is not yet well understood. Outflows are thought to play a role in explaining the phenomenon.

Except for Boroson (2005), all sample studies concentrated on the [O III]–H$\beta$ region of optical spectra of blue outliers in order to examine the phenomenon, while for the first time we include information from all the detected optical NLR lines. We report the detection of strong correlations and discuss consequences for the nature of blue outliers and for dynamical NLR models. This paper is organized as follows. In § 2 we describe the sample selection and provide details on the data analysis. Results on trends and correlations are presented in § 3, which are then discussed in § 4. A summary and conclusions are given in § 5. Some individual objects turn out to be remarkable. Notes on them are provided in the Appendix. We use a cosmology with $H_0 = 70$ km s$^{-1}$ Mpc$^{-1}$, $\Omega_M = 0.3$, and $\Omega_\Lambda = 0.7$ throughout this paper.

## 2. DATA ANALYSIS

### 2.1. *The Sample*

The nine NLS1 galaxies of the present work were drawn from the sample of Xu et al. (2007; D. Xu et al. 2008, in preparation). The original sample selection and standard data reduction procedures were described in detail in that work. In brief, the sample consists of NLS1 galaxies from the catalog of Véron-Cetty & Véron (2003) and a comparison sample of BLS1 galaxies from Boroson (2003) at redshift $z < 0.3$, which have Sloan Digital Sky Survey (SDSS) DR3 (Abazajian et al. 2005) spectra available and which have detectable low-ionization lines (presence of [S II] $\lambda\lambda$6716,6731, with S/N $> 5$). The BLS1 and NLS1 galaxy samples have similar redshift and absolute magnitude distributions. Xu et al. (2007) corrected the SDSS spectra for Galactic extinction, decomposed the continuum into host galaxy and AGN components, and then subtracted the host galaxy contribution and the Fe II complexes from the spectra. Emission-line profiles of the galaxies were fit with Gaussians using the IRAF package SPECFIT (Kriss 1994). Measured FWHMs were corrected for instrumental broadening. Reclassification after spectral emission-line fitting led to 39 BLS1 and 55 NLS1 galaxies in the sample. We focus here on the nine galaxies with the highest blueshifts of [O III] (Table 1) which were identified by KX07. Results from the complete NLS1 (and BLS1) sample are shown for comparison purposes, and in order to identify trends across the whole BLS1–NLS1–blue outlier population. When we report measurements of optical Fe II strength (Fe II $\lambda$4570), this is the integrated flux

TABLE 1
PROPERTIES OF [O III] BLUE OUTLIERS

| Coordinates (J2000.0) (1) | Common Name (2) | $z$ (3) | $\Delta v$ (4) | FWHM ([O III]$_c$) (5) | FWHM (H$\beta_b$) (6) | R5007 (7) | R4570 (8) | $M_{BH}$ (9) | $L/L_{Edd}$ (10) | $n_e$ (11) | $P_{1.4}$ (12) |
|---|---|---|---|---|---|---|---|---|---|---|---|
| 092247.03+512038.0 | SBS 0919+515 | 0.161 | 430 | 720 | 1250 | 0.3 | 1.3 | 6.7 | 1.5 | 10 | |
| 115533.50+010730.6 | SDSS J11555+0107 | 0.198 | 330 | 780 | 1510 | 0.3 | 0.7 | 6.7 | 0.9 | 200 | |
| 013521.68−004402.2 | RX J01354−0043 | 0.099 | 240 | 620 | 1710 | 1.1 | 0.5 | 6.5 | 0.5 | 90 | 22.7 |
| 011929.06−000839.7 | NGC 450-86 | 0.091 | 220 | 380 | 1220 | 0.5 | 0.9 | 6.2 | 0.9 | 200 | |
| 032606.75+011429.9 | SDSS J03261+0114 | 0.128 | 180 | 530 | 1230 | 0.5 | 0.9 | 6.3 | 1.0 | 340 | |
| 120226.76−012915.3 | IRAS 11598−0112 | 0.151 | 170 | 340 | 1460 | 0.5 | 2.7 | 6.8 | 1.1 | 110 | 22.9 |
| 171829.01+573422.4 | SDSS J17184+5734 | 0.101 | 150 | 470 | 1760 | 0.4 | 0.7 | 6.6 | 0.5 | 30 | |
| 124635.25+022208.8 | PG 1244+026 | 0.049 | 150 | 300 | 1200 | 0.6 | 0.8 | 6.2 | 0.9 | 400 | 22.1 |
| 091313.73+365817.3 | RX J09132+3658 | 0.108 | 150 | 350 | 1680 | 1.0 | 0.5 | 6.5 | 0.5 | 40 | 22.5 |

NOTES.—Col. (1): SDSS optical coordinates. Units of right ascension are hours, minutes, and seconds, and units of declination are degrees, arcminutes, and arcseconds. Col. (2): Galaxy name. Col. (3): Redshift determined from H$\beta$. Col. (4): [O III]$_{core}$ velocity ( blueshift) with respect to [S II] in km s$^{-1}$. Col. (5): FWHM([O III]$_c$) in km s$^{-1}$. Col. (6): FWHM(H$\beta_b$) in km s$^{-1}$. Col. (7): Ratio of total [O III] over total H$\beta$ emission. Col. (8): Ratio of Fe II $\lambda$4570 over total H$\beta$ emission. Col. (9): Logarithm of black hole mass in solar masses. Col. (10): Eddington ratio. Col. (11): NLR electron density in cm$^{-3}$. Col. (12): Logarithm of the radio power at 1.4 GHz in W Hz$^{-1}$ of galaxies detected in the *FIRST* survey.

of the Fe II emission complex between the rest wavelengths 4434 and 4684 Å. We refer to the flux sum of the two sulfur lines, [S II] $\lambda$6716 and [S II] $\lambda$6731, as [S II] $\lambda$6725.

### 2.2. *Emission-Line Fits and* [O III] *Profile*

The Balmer lines were decomposed into three components: a narrow core component (H$\beta_n$; FWHM fixed to that determined for [S II] $\lambda\lambda$6716,6731) and two broad components. No physical meaning is ascribed to the two separate broad components; they merely serve as a mathematical description (see D. Xu et al. [2008, in preparation] for alternative Lorentzian fits). The final width of the broad-line emission, H$\beta_b$, is determined as the FWHM of the sum of the two Gaussians. With the exception of [O III], forbidden lines are well represented by single-Gaussian profiles. The total [O III] emission-line profile, [O III]$_{totl}$, was decomposed into two Gaussian components, a narrow core ([O III]$_c$) and a broad base. We distinguish between two types of [O III] spectral complexity: (1) the presence of such a broad base, which tends to be blue-asymmetric (e.g., Heckman et al. 1981) and is referred to as "blue wing"; and (2) systematic blueshifts of the whole core of [O III] (Fig. 2). Objects which show this latter phenomenon are called blue outliers (Zamanov et al. 2002).[1] Measurements of the FWHM and blueshift of [O III] reported in this work refer to the core of the emission line, unless noted otherwise.

Ideally, measurements of the velocity shift of [O III] should be done relative to the galaxy rest frame, as defined by stellar absorption lines from the host galaxy. However, these features are generally weak or absent in our galaxies (and in NLS1 galaxies in general). We therefore measure velocity shifts of [O III] and of all other lines relative to [S II]. We use positive velocity values to refer to blueshifts, and negative ones for redshifts. The shifts of H$\beta$ and other low-ionization lines ([O I] $\lambda$6300, [N II] $\lambda$6584, and [O II] $\lambda$3727) agree well with [S II], while other high-ionization lines ([Ne III] $\lambda$3861, [Ne V] $\lambda$3426, and iron coronal lines) are characterized by high blueshifts (§ 3.3). If lines were too faint to be fit by a Gaussian of free width, we used fixed width instead [fixed to FWHM([S II]) for low-ionization lines or to FWHM([O III]$_c$) for high-ionization lines] and determined the central wavelength to measure the blueshift. Results are reported in Table 1. Since the redshifts provided by the SDSS pipeline are determined based on all strong detected emission lines and are therefore influenced by the blueshifted [O III], we have remeasured redshifts based on H$\beta_n$. It is these redshifts that are given in Table 1. We have measured the average [O III]$_{totl}$/[S II] $\lambda$6725 ratios of our BLS1 and NLS1 galaxy sample. We find that, in terms of this ratio, their NLRs are similar, with $\langle$[O III]$_{totl}$/[S II] $\lambda6725\rangle = 5$ in BLS1 galaxies, and $\langle$[O III]$_{totl}$/[SII] $\lambda6725\rangle = 4$ in NLS1 galaxies.

Notes on individual objects are given in the Appendix. Here we briefly comment on the detection of [Fe X] $\lambda$6375 in two blue outliers. In PG 1244+026 [Fe X] is blended with [O I] $\lambda$6365. For decomposition, the width of [O I] $\lambda$6365 was fixed to that of [O I] $\lambda$6300. The two-component fit then reproduces the expected ratio of [O I] $\lambda$6300/[O I] $\lambda$6365 $\approx 3$. [Fe X] is blueshifted by 640 km s$^{-1}$. In RX J0135−0043, [Fe X] overlaps with atmospheric $O_2$, which is imperfectly corrected for. Therefore, the width of [Fe X] was fixed to that of [O III]. This gives an outflow velocity of 990 km s$^{-1}$.

### 2.3. *Robustness of Spectral Fits: Continuum and Line Decomposition*

In order to see how much the fitting procedure affects measurements of [O III] fluxes, asymmetries, and blueshifts, we have repeated the spectral analysis several times under different conditions and assumptions: We have fit the host galaxy–corrected, Fe II–subtracted spectrum, and for comparison the original SDSS spectrum without any of these corrections. We have refit the [O III] profile in a number of different ways, and with different Gaussian decompositions. The [O III] profile was fit using the red half of the profile only, or different fractions of the total profile, or only the upper 30% of the profile, or with a single- and a double-Gaussian profile. Fitting the profile with one single-Gaussian component maximizes the blueshift in objects with significant [O III] blue wings. In all other cases, uncertainties in line blueshifts due to nonsubtraction of a host galaxy contribution and to different line-fitting procedures are typically much less than 50 km s$^{-1}$. The blueshift independently determined from the weaker line [O III] $\lambda$4959 also agrees with [O III] $\lambda$5007 within better than 50 km s$^{-1}$. Four of our galaxies are also in the sample of Boroson (2005). His [O III] blueshift measurements agree with ours within typically better than $\pm$10 km s$^{-1}$. Uncertainties in FWHM of the core of [O III] are typically 30% for [O III] lines with extra blue wings (smaller in others), and are due to uncertainties in decomposition. We note in passing that the frequency of [O III] blue

[1] Note that we use a velocity shift of $v_{[O\,III]_c} > 150$ km s$^{-1}$ in order to refer to an object as a [O III] blue outlier, while Zamanov et al. (2002) use this terminology for objects with $v_{[O\,III]} > 250$ km s$^{-1}$, where [O III] outflow velocity is measured relative to H$\beta$.

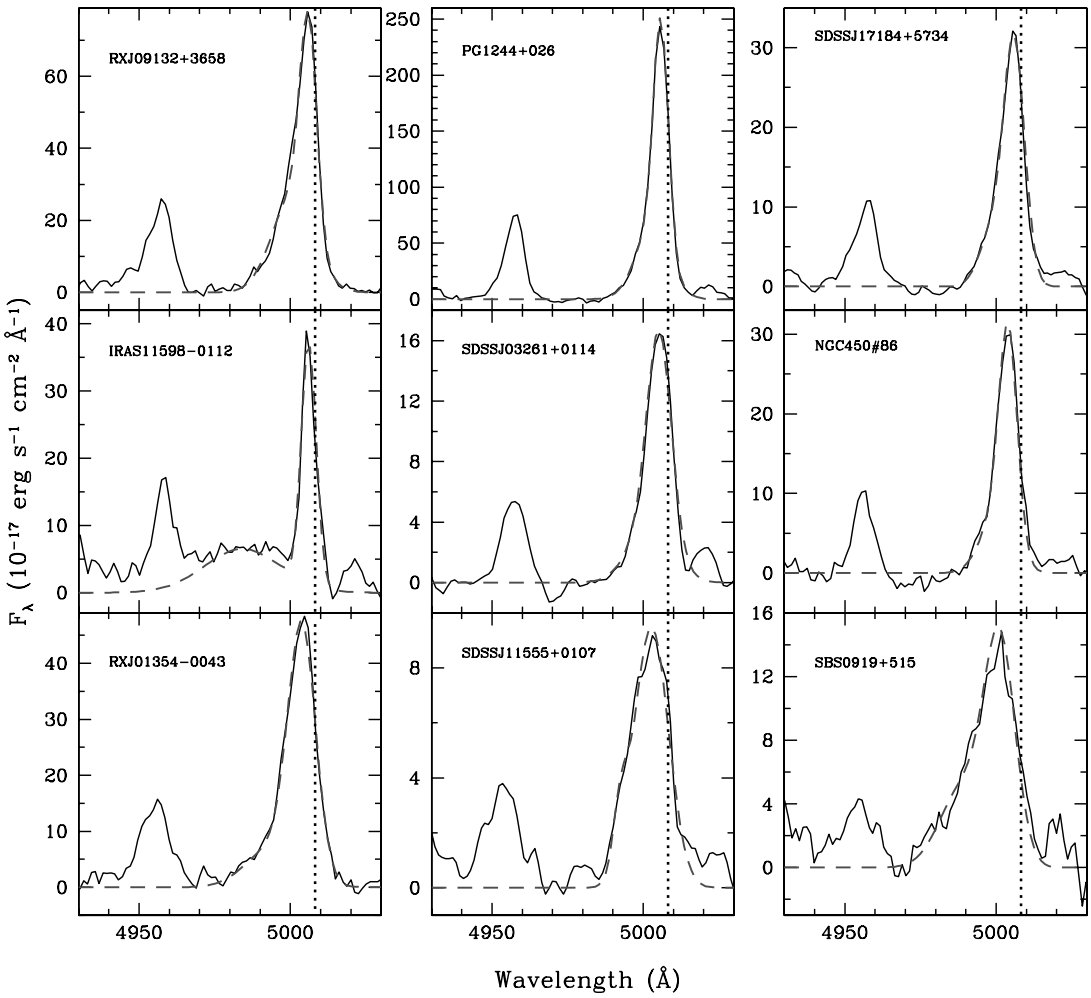


FIG. 2.—[O III] $\lambda\lambda$4959,5007 emission-line region of all nine blue outliers (Fe II– and continuum-subtracted). The expected [O III] peak location according to [S II] is marked with the dotted line. Our two-component Gaussian fit to each [O III] $\lambda$5007 emission line is overplotted using a dashed line. [*See the electronic edition of the Journal for a color version of this figure.*]

wings in blue outliers is neither particularly high nor low (see also Boroson 2005).

## 3. RESULTS

### 3.1. *Constraints on the Presence/Absence of Blueshifted Emission Lines*

In order to facilitate a systematic discussion of NLR models of blue outliers (§ 4.3), we have investigated whether the nonshifted low-ionization lines have a (faint) high-ionization [O III] counterpart and vice versa.[2] We did this representatively for the three galaxies with the highest [O III] blueshifts (SBS 0919+515, SDSS J11555+0107, and RX J01354−0043), and for the galaxy with the highest S/N (PG 1244+026). We have examined the following three questions:

1. Is there any [O III] emission at zero blueshift present in the spectrum (which could originate from the inner NLR, or be a counterpart to the low-ionization emission lines from the outer NLR)? In order to test this, we have enforced an extra Gaussian line contribution to [O III] at zero blueshift (or at $v_{[\mathrm{O\ III}]} = 50$ km s$^{-1}$, the average value of our NLS1 sample excluding blue outliers) and of fixed FWHM($[\mathrm{O\ III}]_{\mathrm{extra}}$) = FWHM([S II]). We find that, if present, it must be very weak. The average ratio $[\mathrm{O\ III}]_{\mathrm{totl}}$/[S II] $\lambda$6725 in our BLS1 sample is 5, while in our NLS1 sample it is 4. This value of 4 is much higher than the upper limit on the extra component which was fit to the observed spectra: typically, $[\mathrm{O\ III}]_{\mathrm{extra}}$/[S II] $\lambda$6725 $\approx$ 0.1–0.4, and always, $[\mathrm{O\ III}]_{\mathrm{extra}}$/[S II] $\lambda$6725 $< 1$. Since the ratio of [O III]/[S II] of nearby Seyfert galaxies generally decreases in dependence of radius (in models and observations; Komossa & Schulz 1997; Bennert et al. 2006), and since there must be an [O III] contribution from the outer [S II]–emitting clouds, the limits derived on any nonblueshifted [O III] contribution from the *inner* NLR are very tight.

2. Does the blueshifted [O III] have a blueshifted H$\beta$ counterpart? That is, how much highly blueshifted H$\beta$ could be "hidden" in the H$\beta$ profile? In order to check this, we have refit H$\beta$ adding an additional Gaussian to describe its profile with parameters of this extra component fixed at $v_{\mathrm{H}\beta_{\mathrm{extra}}} = v_{[\mathrm{O\ III}]_c}$, FWHM($\mathrm{H}\beta_{\mathrm{extra}}$) = FWHM($[\mathrm{O\ III}]_c$), and an intensity ratio $[\mathrm{O\ III}]_c/\mathrm{H}\beta_{\mathrm{extra}} = 10$. We find that such a weak component could generally be hidden in the H$\beta$ profile.

3. Does the blueshifted [O III] have a blueshifted low-ionization counterpart in [S II]? This is not the case. For typical *spatially averaged* ratios of [O III]/[S II] $\lambda$6725 $\approx$ 4 of our NLS1 sample, blueshifted [S II] lines would have generally been detectable, but

[2] Note that, apart from [O III], other high-ionization lines show blueshifts too (§ 3.3.1), but they are too faint for multicomponent line decompositions. Among the nonshifted emission lines, [S II] is the strongest unblended line, and we therefore focus on [S II] for the corresponding estimates in this section.

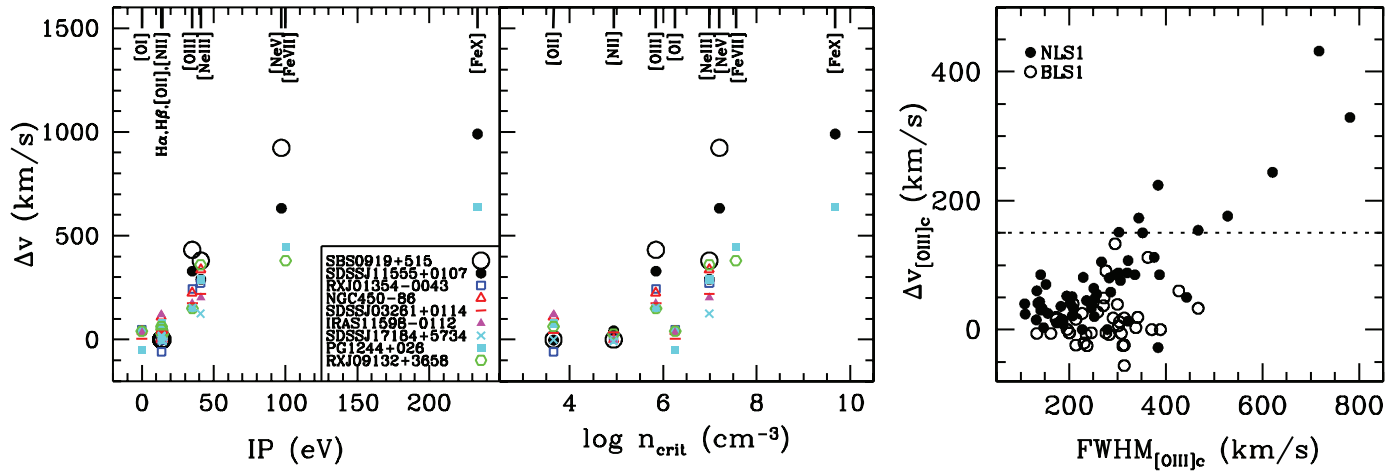


FIG. 3.— Velocity shift of individual emission lines vs. the ionization potential IP and the critical density $n_{crit}$ (*left*), and correlation of the [O III] line width with the [O III] blueshift (*right*).

are absent. Very faint blueshifted [S II], as it may arise in the *inner* NLR, cannot be excluded with the present data.

In summary, we find (1) little evidence for zero-blueshift [O III] emission (the amount of emission consistent with the spectra likely originates from the outer parts of the NLR which also emits in [S II] and other low-ionization lines); (2) that an extra blueshifted component in H$\beta$—the expected counterpart to blueshifted [O III]—can be hidden in the H$\beta$ profile; and (3) that there is no detectable highly blueshifted component in the low-ionization lines.

### 3.2. *Estimates of Black Holes Masses, Eddington Ratios, and NLR Densities*

Black hole masses were estimated by using the radius-luminosity ($R_{BLR}$-$L$) relation of BLS1 galaxies as reported by Kaspi et al. (2005) and the width of H$\beta$. The luminosities at 5100 Å were taken from D. Xu et al. (2008, in preparation) and are based on SDSS $g^*$ and $r^*$ magnitudes corrected for Galactic extinction. Since we lack multiwavelength spectral energy distributions, the bolometric luminosity $L_{bol}$ was estimated using a standard bolometric correction of $L_{bol} = 9\lambda L_{5100}$ (Kaspi et al. 2000). The value of $L_{Edd}$ was calculated from the black hole mass, according to $L_{Edd} = 1.3 \times 10^{38}\, M_{BH}/M_{\odot}$ erg s$^{-1}$. Typical errors in individual BH mass estimates can be as large as 0.5 dex, and arise from the use of single-epoch data, and uncertainties in H$\beta$ decomposition and in host galaxy contribution. The NLR density was derived from the density-sensitive [S II] intensity ratio, [S II] $\lambda$6716/[S II] $\lambda$6731 (Xu et al. 2007).

### 3.3. *Trends and Correlations*

We have checked for (1) trends of outflow velocity with other (atomic) parameters within each single spectrum, and (2) for trends across our sample of blue outliers (do all blue outliers have high Eddington ratios, high black hole masses, etc.?), and (3) for trends across our whole sample of BLS1 and NLS1 galaxies.

#### 3.3.1. *A Strong Correlation of Line Shift with Ionization Potential*

We detect a strong correlation between emission-line blueshift and ionization potential (Fig. 3). While the low-ionization forbidden lines of [O I], [O II], and [N II], and the Balmer lines H$\alpha$ and H$\beta$, are at velocities very similar to [S II], high-ionization lines, on the other hand, show strong blueshifts which increase with ionization potential. Two galaxies (SDSS J115533.50+010730.4 and PG 1244+026) show extreme blueshifts in [Fe X], on the order of 600–1000 km s$^{-1}$. There is also a correlation between outflow velocity and critical density of the individual line transitions (Fig. 3), but it is less tight in the sense that [O I] $\lambda$6300, which has low ionization potential but high critical density, does not follow the trend.

#### 3.3.2. *Trends and Correlations of* [O III] *Blueshift with Line and Galaxy Parameters*

We have correlated the [O III] blueshifts (of the blue outliers, and of our sample as a whole) with various other line parameters (e.g., line widths and line ratios) and with galaxy properties (absolute magnitude, black hole mass, Eddington ratio, and NLR density). The strongest correlation is the one between [O III] blueshift and [O III] line width (Spearman rank correlation coefficient $r_S = 0.6$ for the whole NLS1 sample and even higher for just the blue outliers; Fig. 3). Within the NLS1 sample, there is a trend that blue outliers preferentially avoid low Eddington ratios $L/L_{edd}$ and low Fe II/H$\beta$ ratios. Most blue outliers have small ratios of [O III]/H$\beta_{totl}$. We do not find trends of outflow velocity with NLR density $n_e$, black hole mass, absolute magnitude $M_i$, and the width of the broad component of H$\beta$ (Fig. 4). However, while trends are absent within the NLS1 population itself, it is interesting to note that the presence of blue outliers amplifies trends which become apparent when the BLS1 galaxies are added to the correlation plots (Fig. 4).

### 3.4. *Frequency of Blue Outliers*

Among our sample, blue outliers only occur in NLS1 galaxies. At a velocity $v_{[O\,III]} \gtrsim 150$ km s$^{-1}$, we have a blue outlier fraction of 16%. If we use $v_{[O\,III]} \gtrsim 250$ km s$^{-1}$ instead, as in Zamanov et al. (2002), the fraction of blue outliers among NLS1 galaxies is 5%.

## 4. DISCUSSION

### 4.1. *The Locus of Seyfert Galaxies with* [O III] *Blueshifts on the $M_{BH}$-$\sigma$ Plane*

Investigating the location of different types of galaxies on the $M_{BH}$-$\sigma$ plane, and their potential evolution across the plane, is of great interest in the context of galaxy formation and evolution models. In AGNs, stellar velocity dispersion is often difficult to measure, and the width of [O III] has become a convenient proxy for stellar velocity dispersion (e.g., Terlevich et al. 1990; Whittle

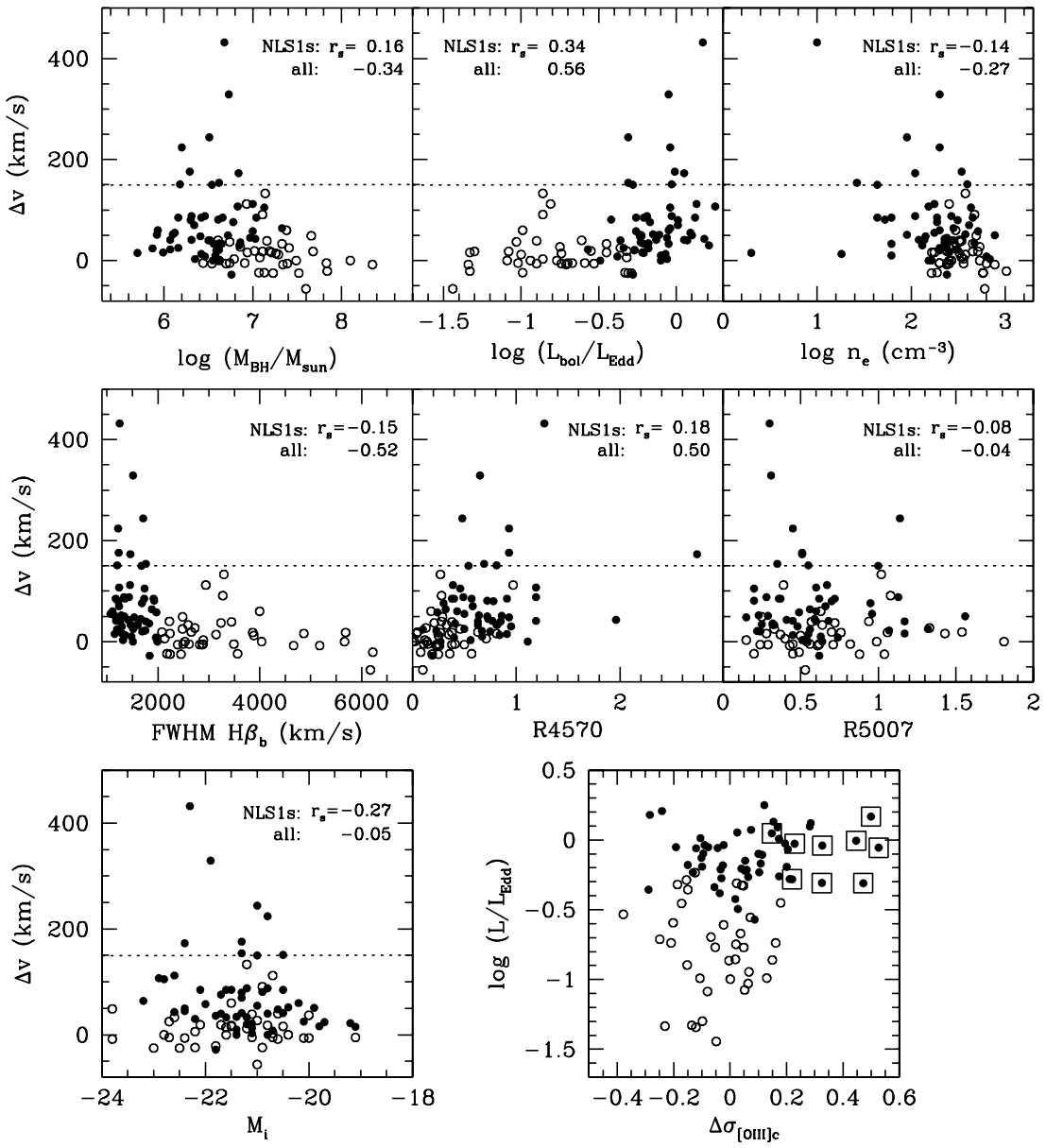


FIG. 4.—Correlation of [O III] outflow velocity with other emission-line and AGN properties (first panel to seventh panel). Objects above the dashed line are blue outliers. NLS1 galaxies are represented by filled circles, and BLS1 galaxies by open circles. The correlation coefficient $r_s$ shown in each panel was calculated among the NLS1 population only, or for the whole sample (marked as "all" in the graphs). If the BLS1 galaxies are included, several correlations emerge, and the blue outliers amplify these trends. R5007 corresponds to the ratio of total [O III] over total H$\beta$ emission, R4570 to the ratio of Fe II $\lambda$4570 over total H$\beta$ emission. The last panel shows the galaxies' deviation $\Delta\sigma$ (see text for definition) from the $M_{BH}$-$\sigma_*$ relation, in dependence of Eddington ratio. An apparent correlation does no longer exist once the blue outliers (marked with extra open squares) are removed.

1992; Nelson & Whittle 1996; Nelson 2000; Shields et al. 2003; Boroson 2003; Greene & Ho 2005; Netzer & Trakhtenbrot 2007; Salviander et al. 2007) after removing [O III] blue wings and excluding galaxies with powerful kiloparsec-scale linear radio sources. The scatter in the relation is larger than in the original $M_{BH}$-$\sigma_*$ relation (Ferrarese & Merritt 2000; Gebhardt et al. 2000), and indicates secondary influences on the gas kinematics (e.g., Nelson & Whittle 1996; Rice et al. 2006).

Mathur et al. (2001) pointed out the importance of studying the locus of NLS1 galaxies on the $M_{BH}$-$\sigma$ plane, which was the focus of a number of subsequent studies (Wang & Lu 2001; Wandel 2002; Botte et al. 2004, 2005; Bian & Zhao 2004; Grupe & Mathur 2004; Barth et al. 2005; Greene & Ho 2005; Mathur & Grupe 2005a, 2005b; Zhou et al. 2006; Ryan et al. 2007; Watson et al. 2007; KX07). Any such study would involve one important step: the distinction between true outliers from the $M_{BH}$-$\sigma$ relation on the one hand, and apparent outliers on the other hand. Apparent outliers would only appear to be offset from the $M_{BH}$-$\sigma$ relation because either the choice of line width as a measure of stellar velocity dispersion was unsuitable, or the choice of line and continuum parameters as a measure of black hole mass was unsuitable. KX07 have shown that those NLS1 galaxies of their sample which deviate significantly from the $M_{BH}$-$\sigma$ relation of normal (and BLS1) galaxies are all characterized by high [O III] blueshifts. While these [O III] lines were therefore not suited as surrogates for stellar velocity dispersion, the [S II]–based measurements of velocity dispersion of the very same objects still located them on the $M_{BH}$-$\sigma$ relation. Almost all galaxies which deviate most strongly from the $M_{BH}$-$\sigma$ relation (see our Fig. 1) show $v_{[O\,III]} > 150\,km\,s^{-1}$. These six objects, plus three additional ones

which also show $v_{[O\ III]} > 150$ km s$^{-1}$, define the nine blue outliers that are the target of the present study.

In order to measure systematically the deviation of a galaxy from the $M_{BH}$-$\sigma_*$ relation, we define the quantity $\Delta\sigma \equiv \log \sigma_{obs} - \log \sigma_{pred}$ (as in KX07), where $\sigma_{obs}$ is the observed emission-line velocity dispersion and $\sigma_{pred}$ is the stellar velocity dispersion predicted from the $M_{BH}$-$\sigma_*$ relation of Ferrarese & Ford (2005). We find a strong correlation between [O III] blueshift $v_{[O\ III]}$ and $\Delta\sigma$ (Fig. 1). This finding demonstrates that a [O III] velocity shift systematically affects the deviation of an object from the $M_{BH}$-$\sigma$ relation (see also Boroson 2005). We further find that a correlation between $L/L_{Edd}$ and $\Delta\sigma$ (e.g., Mathur & Grupe 2005a; Greene & Ho 2005; see also Netzer & Trakhtenbrot 2007) is only present in our sample if we include blue outliers; when they are removed from the sample, no correlation remains (Fig. 4, *last panel*; see also KX07).

Two of our NLS1 blue outliers have independent BH mass estimates. From X-ray variability, Czerny et al. (2001) estimated $\log M_{BH} = 5.9$ for PG 1244+062, which agrees well with our estimate from applying the $R_{BLR}$-$L$ relation ($\log M_{BH} = 6.2$). For RX 01354−0043 we directly measured $\sigma_*$ from stellar absorption lines (see Appendix). The value agrees well with $\sigma_{[S\ II]}$ and puts RX J01354−0043 almost perfectly on the $M_{BH}$-$\sigma_*$ relation (Fig. 1).

These findings demonstrate the importance of measuring [O III] blueshifts and removing objects with high blueshifts from a sample before putting it on the $M_{BH}$-$\sigma_{[O\ III]}$ relation. The independent question arises as to what may cause the blueshifts of these [O III] outliers.

### 4.2. *Blue Outliers: Trends and Correlations*

The phenomenon of slightly different blueshifts and line widths of NLR emission lines has been recognized since the early days of AGN spectroscopy and is generally traced back to a certain stratification of the NLR in the sense that high-ionization lines are produced preferentially at small distances from the core, while low-ionization lines are preferentially produced at larger radii (e.g., Osterbrock 1991). The presence of a strong [O III] blueshift on the order of several hundred km s$^{-1}$ was noticed early in the prototype NLS1 galaxy I Zw 1[3] (e.g., Phillips 1976; Véron-Cetty et al. 2004). The galaxy also shows very blueshifted IR coronal lines (Schinnerer et al. 1998) and blueshifted UV high-ionization broad lines (Laor et al. 1997).

Several recent studies systematically examined the phenomenon of blue outliers in larger samples of type 1 Seyfert galaxies (Zamanov et al. 2002; Marziani et al. 2003; Aoki et al. 2005; Boroson 2005; Bian et al. 2005). According to these studies blue outliers have high Eddington ratios and small BLR Balmer line widths. However, not all sources with high Eddington ratios are blue outliers. While Bian et al. (2005) further reported a correlation between blueshift and Eddington ratio of their seven blue outliers, Aoki et al. (2005) did not find such a correlation for 16 objects. A strong correlation between [O III] blueshift and [O III] line width is often seen, and is usually interpreted as evidence for outflows. Zamanov et al. (2002) noticed that most of their blue outliers also show high blueshifts in C IV $\lambda$1549 (but this phenomenon is not exclusive to blue outliers; Sulentic et al. 2007). Aoki et al. (2005) reported a trend that blue outliers have high black hole masses ($>10^7\ M_\odot$). All previous studies of samples of blue outliers focused on the [O III]–H$\beta$ spectral region in order to explore the phenomenon, with the exception of Boroson (2005). Although Boroson (2005) measured the positions of other NLR lines in order to establish a systemic reference for the [O III] line properties, we have, for the first time, measured the widths and strengths of all the optical NLR lines in blue outliers in order to study the nature of blue outliers and explore the dynamics of the NLR.

For each galaxy, we find a strong correlation between emission-line blueshift and ionization potential of the line-emitting ion. Coincidentally, higher ionization potentials of the ions in question also come with higher critical densities of the forbidden line transitions observed from the respective ions. Therefore, a correlation between outflow velocity and ionization potential would generally imply a correlation with critical density, and vice versa, raising the question of which of the two is the fundamental correlation: density stratification or ionization stratification. An important exception to the above rule is [O I] $\lambda$6300, which has zero ionization potential, while its critical density ($n_{crit} = 1.8 \times 10^6$ cm$^{-3}$) is relatively high. [O I] is detected in several of our NLS1 galaxies, and we find that [O I] follows the trend in ionization potential, but not in critical density, arguing that the former correlation is the underlying one (Fig. 3).[4] We confirm the previously known correlation between [O III] blueshift and line width.

Blue outliers only occur among the NLS1 galaxies of our sample (i.e., sources with high Eddington ratios and small Balmer line widths), but within the NLS1 population blue outliers do not show a strong correlation with Eddington ratio even though they preferentially avoid low ratios. No correlation of outflow velocity with black hole mass, absolute magnitude, and the width of the broad component of H$\beta$ is found. Like in other samples, the number of objects is small, and larger samples of blue outliers are needed to confirm the weak trends.

It has occasionally been suggested that [O III] in blue outliers appears broadened by orientation effects in the sense that we look face-on at the central engine, and into an outflow (Zamanov et al. 2002; Marziani et al. 2003; Boroson 2005). If that scenario is correct, we can use blue outliers as test beds for orientation-dependent models of NLS1 galaxies which allow for the possibility that the H$\beta$ line of NLS1 galaxies is narrowed due to viewing angle effects. If, in blue outliers, the BLR were in a plane and if we viewed it face-on, blue outliers should have the smallest H$\beta$ widths among NLS1 galaxies (here we temporarily classify NLS1 galaxies independently of their H$\beta$ width, but only use the ratios [O III]/H$\beta$ and Fe II/H$\beta$, which still makes all of our blue outliers NLS1 galaxies: in all cases [O III]/H$\beta_{totl} < 3$, and Fe II/H$\beta_{totl} > 0.5$). However, we do not find any trend for small widths of the broad Balmer lines among the objects of our sample (see Fig. 4).

The [O III] lines of several objects still show the phenomenon of blue wings, arguing against the previous suggestion that the classical [O III] emission in blue outliers is absent and we actually only see the blue wing. (However, occasionally the presence of a strong blue wing could mimic a blue outlier, if the wing were not spectroscopically resolved from the core of the line [e.g., Grandi 1977; Holt et al. 2003.])

### 4.3. *Models of the Narrow-Line Region*

There is good evidence that the motion of NLR clouds is strongly influenced by the bulge gravitational potential (e.g., Véron 1981; Whittle 1992; Nelson & Whittle 1996; see § 4.1). At

[3] It is also known in some radio galaxies (e.g., PKS 1549−79 [Tadhunter et al. 2001; Holt et al. 2006], IC 5063 [Morganti et al. 2007], and PKS 0736+01 [Zamanov et al. 2002; Marziani et al. 2003]). Also note systematic blueshifts in high-ionization BLR emission lines in quasar samples (e.g., Gaskell 1982; Sulentic et al. 2007).

[4] It is well possible that we have both ionization and density stratification. In that case, the inner high-density clouds are also highly ionized and/or matter-bounded, with little [O I] left.

the same time, there is also evidence for radial motions in NLRs based, for instance, on blue asymmetries of [O III] profiles (e.g., de Robertis & Osterbrock 1984; Veilleux 1991; Whittle 1992; Véron-Cetty et al. 2001), on correlations of blue wing blueshift with the Eddington ratio and other arguments (Xu et al. 2007), and on spatially resolved [O III] velocity shifts (e.g., Schulz 1990; Das et al. 2005). The existence of [O III] blue wings can formally be equally well interpreted in terms of inflows or outflows, plus selective obscuration. Generally, there is a preference for the outflow interpretation.

Regarding theoretical models for outflows, a lot of work has focussed on magnetocentrifugal winds and radiatively driven outflows from the accretion disk region (see Königl 2006; Everett 2007; Proga 2007 for reviews). These models have successfully been applied to BAL flows and the BLR emission lines, are supported by recent observations (Young et al. 2007), and have recently been extended to spatial scales typical of the very inner NLR (Proga et al. 2008). However, little is known about the formation or continuation of such winds on much larger scales on the order of 100 pc to kiloparsec characteristic for NLRs. Mechanisms suggested to be relevant in the NLR (and CLR) include radiation pressure acting on gas (Binette et al. 1997; Das et al. 2007) and on dust grains embedded in the clouds (Binette 1998; Dopita et al. 2002), and the entrainment of NLR clouds in hot winds (Krolik & Vrtilek 1984; Schiano 1986; Mathews & Veilleux 1989; Smith 1993; Everett & Murray 2007). The presence of collimated outflows of radio plasma in the form of jets and their local interaction with NLR clouds has been observed directly (e.g., Falcke et al. 1998). Spatially resolved imaging spectroscopy of nearby AGNs has produced several good examples of spatial coincidences between radio jets and line blueshifts (e.g., Riffel et al. 2006; Morganti et al. 2007), while in other cases the jet-cloud interaction is very weak and does not significantly affect the local NLR velocity field (e.g., Cecil et al. 2002; Das et al. 2005). In some cases, jets are absent but emission lines are still blueshifted (F. K. B. Barbosa et al. 2008, in preparation). In AGNs with strong starburst activity winds could also be starburst driven (e.g., Rupke et al. 2005).

Regarding NLS1 galaxies, their high Eddington ratios make the presence of radiation-pressure driven *winds* (on the accretion disk scale) very likely. Less certain and understood is the efficiency of *jet* launching under high accretion rate conditions. Again, these mechanisms refer to the innermost AGN region, not to larger scales. Blue outliers with their extreme velocity shifts place particularly tight constraints on models for AGN outflows on large, i.e., NLR, scales. We discuss several NLR models for blue outliers in turn.

#### 4.3.1. *A Compact NLR?*

Zamanov et al. (2002) and Marziani et al. (2003) suggested that blue outliers posses a very compact NLR, perhaps the result of the youth of those NLS1 galaxies which did not yet develop a full NLR. Their idea was based on the assumption that blue outliers would only posses [O III] emission and lack other narrow emission lines. However, we do find a classical NLR in terms of the presence of low-ionization lines. Furthermore, the fact that their [S II] line widths put the blue outliers on the same $M_{\rm BH}$-$\sigma$ relation with BLS1 and normal galaxies strongly indicates that their outer NLR is a quiescent classical NLR similar to that of other BLS1 and NLS1 galaxies.

#### 4.3.2. *A Two-Component NLR*

The strong blueshifts we detect in the high-ionization component raises the possibility that we see two independent components: a classical NLR, plus an independent outflow component which could be due to a disk wind, a wind from the torus, or in the form of a lowly ionized warm absorber. However, this interpretation is very unlikely, because the nonblueshifted [O III] counterpart to the low-ionization lines, as would be expected from *the inner part* of a classical NLR, is weak or absent. This fact leads us almost inevitably to the third and fourth possibilities.

#### 4.3.3. *A Classical NLR, Modified at Small Radii*

The fact that we do not detect a classical inner NLR, in the form of a second, nonblueshifted [O III] emission component, implies that processes directly modify/disturb at least the inner NLR, perhaps in the form of a radio jet–cloud interaction. However, the strong dependence of emission-line velocity shift on ionization potential that we detect (Fig. 3) indicates that we see a highly stratified, photoionized medium, not a local interaction due to shocks and locally disturbed velocity fields.

#### 4.3.4. *NLR Clouds Entrained in a Wind*

The phenomenologically most straightforward solution is one in which the (CLR and) NLR clouds themselves follow a decelerated outflow. This scenario requires an efficient driving mechanism and perhaps an efficient deceleration mechanism. One possibility is direct acceleration of the NLR clouds by radiation pressure acting on gas or dust; another is the presence of a hot wind which entrains the NLR clouds (see § 4.4). If the wind forms a decelerating outflow, the entrained clouds of the CLR/inner NLR would have the highest outflow velocities, respectively, which would decrease in dependence of core distance and would leave the outer, low-ionization part of the NLR unaffected.

Zamanov et al. (2002) reported a linkage of [O III] "blue outlierness" with broad-line C IV blueshift. Could the same wind persist from the disk, to the high-ionization BLR (but leave the bulk of the BLR unaffected, possibly by blowing perpendicular), and on to the CLR and inner NLR?

In this picture, the NLRs of BLS1 galaxies, NLS1s, and blue outliers would be intrinsically similar, and the motion of NLR clouds generally dominated by the bulge gravitational potential. Which emission-line regions partake in an outflow would depend on the efficiency/operating distance of the wind. It could be present in all AGNs, but would generally only affect the CLR (in AGNs with blueshifted iron coronal lines but quiescent NLRs), or level off even before reaching the CLR.

### 4.4. *Mechanisms of Cloud Acceleration and Entrainment*

While phenomenologically successful, the question is raised as to the origin of the wind/outflow on the one hand, and the entrainment mechanism and cloud stability against disruptive instabilities (Mathews & Veilleux 1989; Schiano et al. 1995) on the other hand. We discuss several possibilities in turn.

*Cloud acceleration by radiation pressure acting on dust.*—Radiation pressure acting on dust grains embedded in the gas clouds is an efficient method of cloud acceleration (e.g., Binette 1998; Dopita et al. 2002; Fabian et al. 2006). In blue outliers, this mechanism is likely not at work, because we do not expect dust in the high-ionization BLR (we are assuming here that the high-ionization part of the BLR partakes in the outflow, motivated by the results of Zamanov et al. [2002] described in § 4.3.4). Some dust might be present in the CLR (even a small admixture of dust would still lead to efficient radiative acceleration, and generally still predict sufficiently strong gas-phase iron lines; Binette 1998). While, observationally, dust-rich NLRs could be present in individual blue outliers (e.g., RX J0135−0043), most of them have very blue optical continua, arguing against the presence of

an excess of dusty gas along the line of sight. These arguments make cloud acceleration by radiation pressure acting on dust grains an unlikely scenario.

*Cloud entrainment in collimated radio plasma*.—Outflowing radio plasma in the form of jets is known to be present and to reach large distances from the nucleus in AGNs, so could plausibly affect several emission-line regions on its way. The phenomenon of cloud entrainment in radio plasma has been directly observed and studied in star-forming regions (Ostriker et al. 2001; Stojimirović et al. 2006). Jet-cloud interaction can result in a variety of phenomena, including cloud entrainment, jet deflection and disruption, and cloud destruction (e.g., Saxton et al. 2005; Krause 2007 and references therein). Of interest here is entrainment (Blandford & Königl 1979; Schiano et al. 1995; Fedorenko et al. 1996). One key problem is cloud longevity against various instabilities. Fedorenko et al. (1996) argued for magnetic NLR confinement, which would then allow for NLR cloud entrainment in radio jets.

Independent of theoretical considerations the question is raised if the blue outliers of our sample all harbor powerful radio jets. Relatively little is known about the radio properties of NLS1 galaxies in general. On average, they tend to be less radio-loud than BLS1 galaxies (Zhou et al. 2006; Komossa et al. 2006) and share some similarities with compact steep-spectrum radio sources (Komossa et al. 2006). Four of the blue outliers of our sample have *FIRST* radio detections. These imply radio powers of $P_{1.4} = 10^{22}$ to $8 \times 10^{23}$ W Hz$^{-1}$ (Table 1) at 1.4 GHz; similar to those AGNs which Nelson & Whittle (1996) find to be offset from the $M_{\rm BH}$-$\sigma_*$ relation. We do not have information on the radio morphology of the blue outliers. Sources are unresolved with *FIRST*, with one remarkable exception: the radio emission of RX J0135−0043 is extended by ∼10 kpc (or double; see Appendix). Spatially resolved radio observations of the sources are required to search for the presence of jets and to study the radio properties in more detail.

*Thermal winds*.—Variants of thermal wind models have been studied in order to explain the kinematics of ionized absorbers (Chelouche & Netzer 2005), and of NLRs. *Isothermal* Parker wind models of Everett & Murray (2007), originally computed in order to model spatially resolved NLR velocity gradients of NGC 4151 (Das et al. 2005), would have roughly the right properties to explain our average blue outlier velocity shifts and radial velocity changes. A range in NLR cloud column densities would lead to a spread in cloud velocities (see eq. [10] of Everett & Murray 2007), thereby perhaps explaining the observed line broadening. However, as also shown by Everett & Murray (2007), realistic models including photoionization heating have temperature gradients, and adiabatic cooling decelerates the winds too quickly. An extra heating source of unknown nature would be needed in order to keep the wind isothermal. The models of Das et al. (2007), based on the radiative acceleration of NLR clouds, implied that NLR clouds do not decelerate quickly enough in order to explain NLR velocity gradients of NGC 1068 observed with *HST*; models work after introducing drag forces from an ambient medium. Detailed modeling of the present data would likely involve several of the above model ingredients. Such modeling is beyond the scope of this paper.

*High Eddington ratios and orientation effects*.—Common to blue outliers is their high Eddington ratios. Could high $L/L_{\rm Edd}$ be the wind-driving mechanism? Additional orientation effects (as also discussed by Marziani et al. 2003; Boroson 2005) are still needed in order to explain why not all AGNs with high $L/L_{\rm Edd}$ are blue outliers. Near face-on orientation would have us look more down the flow in blue outliers, thereby enhancing the stratification, broadening, and blueshift effect.

### 4.5. *Links with* (*Compact*) *Radio Sources and Mergers*

It is interesting to point out similarities between the phenomenon of blue outliers in NLS1 galaxies and in radio galaxies (see also Holt et al. 2006). Several radio galaxies show a similar phenomenon of high [O III] core blueshifts and line broadening (e.g., Tadhunter et al. 2001; Marziani et al. 2003; Holt et al. 2006; Stockton et al. 2007; see Gupta et al. 2005 for a related phenomenon in the UV). Jet-cloud interaction in the (inner) NLR is the favored interpretation of most of these sources. These objects may represent the early stages of radio-source evolution (Tadhunter et al. 2001). Radio galaxies with blue outliers in [O III] are typically compact flat-spectrum sources, are absorbed, and are luminous in the infrared. For some (e.g., PKS 1549−79 and PKS 0736+01) there is evidence that we have a near face-on view (Tadhunter et al. 2001; Marziani et al. 2003). As pointed out before, the strong stratification we see in NLS1 blue outliers argues against local jet-cloud interactions in those galaxies, but would be consistent with NLR clouds entrained in the outflowing radio plasma.

The blue outliers among the radio galaxies show signs of recent mergers. Regarding NLS1 galaxies in general, there is no evidence that the majority of them underwent recent mergers or have an excess of companion galaxies (Krongold et al. 2001; Ryan et al. 2007). Little is known about the host galaxies of our blue outlier sample, in particular. IRAS 11598−0112 indeed is a merger with prominent tidal tails (Veilleux et al. 2002), ultraluminous in the infrared. Inspecting the SDSS images of the other galaxies of our sample we do not find strongly disturbed galaxy images indicating ongoing mergers, but this needs to be confirmed with deeper imaging. One galaxy, RX J0135−0043, shows indications of an off-center nucleus. That effect could be caused by interaction, be mimicked by dust, or have another origin.

### 4.6. *Recoiled Black Holes?*

Recent simulations of merging black holes predict black hole recoil velocities due to emission of gravitational wave radiation up to several thousand km s$^{-1}$ (e.g., Campanelli et al. 2007; review by Pretorius 2007). Potentially, high relative outflow velocities of AGN emission-line regions versus the host galaxy can arise if the recoiled black hole keeps its BLR and inner NLR (Bonning et al. 2007). Applied to blue outliers, if they harbored recoiled BHs, their whole BLR (plus the high-ionization NLR) should show high blueshifts, while the "remnant" NLR would still appear in low-ionization lines. In that case, we expect the broad component of the Balmer lines to exhibit the highest blueshifts of all emission lines; this is, however, not observed. Shifts in broad H$\beta$ are less than those in [O III].

### 4.7. *Future Work*

The SDSS database is well suited for a systematic search for more blue outliers. Zhou et al. (2006) mention in passing the presence of several extreme ones among their NLS1 galaxy sample but do not discuss them further. Spatially resolved optical spectroscopy will allow us to measure directly line widths, outflow velocities, etc., in dependence of the core distance.[5] Spectroscopy in the IR and UV will tell whether trends (a correlation with ionization potential) persist in IR coronal lines and high-ionization

[5] This approach is difficult, however, if the near-pole-on interpretation of blue outliers is correct.

UV broad lines. X-ray measurements of blue outliers will be useful to search for signs of high-velocity ionized outflows, and to see whether blue outliers again stick out in AGN correlation space when adding their X-ray properties (X-ray steepness, variability) to correlation analyses. Radio observations (at high resolution) of all galaxies will facilitate further comparison between blue outliers in radio galaxies and NLS1 galaxies and will tell whether radio jets are present in NLS1 blue outliers. Radio observations have the potential to confirm the pole-on hypothesis of blue outliers, if relativistic beaming is detected. Imaging with *HST* will reveal whether the host galaxies of blue outliers show signs of recent mergers. In particular, galaxy merger simulations predict strong outflows in the final merger phase (e.g., Springel et al. 2005). Imaging will allow us to test whether blue outliers are in such a phase.

If the face-on interpretation of blue outliers is correct, they are also useful test beds for the question of whether the width of broad H$\beta$ is systematically affected by orientation. Increasing the sample size will allow us to test more stringently whether the broad component of H$\beta$ is systematically narrower in blue outliers. If so, this would imply that BLR clouds are arranged in a plane, and we would underestimate systematically the BH masses in these objects, and perhaps NLS1 galaxies in general. If, instead, their BLR is spherical, we would not see systematically narrower H$\beta$ in objects viewed face-on, and would not have to worry about the correctness of BH mass estimates. Our preliminary results indicate that the latter is the case.

On the theoretical side, the question is raised as to which winds can operate across long distances spanning the high-ionization BLR, CLR, and a substantial part of the NLR, predict the observed gradient in cloud velocities ($\sim$1000 km s$^{-1}$ of high-ionization emission-line clouds close to the nucleus, and several hundred km s$^{-1}$ farther out on typical NLR scales, while the outer NLR is mostly unaffected), and ensure the longevity of the emission-line clouds.

## 5. SUMMARY AND CONCLUSIONS

In [O III] blue outliers with their extreme velocity shifts the effects of secondary influences on the NLR kinematics are enhanced or dominate completely. Their study is therefore of great relevance for (1) scrutinizing the usefulness and limitations of [O III] width as a proxy for stellar velocity dispersion; (2) understanding the origin and dynamics of the NLR; (3) investigating driving mechanisms of AGN outflows on large scales; and (4) examining possible links with results from merger simulations which predict that a substantial fraction of the ISM of the merger should be outflowing. We have systematically studied the optical properties of such AGNs with high [O III] blueshifts which deviate from the $M_{\rm BH}$-$\sigma_{\rm [O\,III]}$ relation of BLS1 and NLS1 galaxies, and obtained the following results:

1. All of them have high Eddington ratios ($L/L_{\rm edd} = 0.5$–$1.5$) and narrow BLR Balmer lines [FWHM(H$\beta_b$) = 1200–1800 km s$^{-1}$], which makes them NLS1 galaxies. The fraction of blue outliers among our NLS1 sample is 16% ($v_{\rm [O\,III]} \gtrsim 150$ km s$^{-1}$), and 5% at the highest outflow velocities ($v_{\rm [O\,III]} \gtrsim 250$ km s$^{-1}$). While blue outliers do enhance correlations which appear across the whole BLS1-NLS1 population, we do not find strong correlations of [O III] outflow velocity with the Eddington ratio within the blue outlier population itself, perhaps due to the small sample size.

2. We do detect a strong correlation between emission-line blueshift and ionization potential, and confirm a strong correlation between [O III] blueshift and [O III] line width. The presence of a classical quiescent *outer* NLR is indicated by the existence of low-ionization lines, by [S II] line widths which locate the blue outliers on the same $M_{\rm BH}$-$\sigma_{\rm [S\,II]}$ relation as other BLS1 and NLS1 galaxies, and by inferred NLR densities similar to other NLS1 galaxies. On the other hand, zero-blueshift [O III] emission expected from a quiescent *inner* NLR is weak or absent.

3. Taken together, these observations place tight constraints on models: We favor a scenario where NLR clouds of blue outliers are entrained in a decelerating wind. Similar, less powerful winds could be present in all AGNs, but would generally only affect the CLR (in AGNs with blueshifted iron coronal lines but quiescent NLRs), or level off even before reaching the CLR only affecting the high-ionization BLR.

4. The mechanism that drives and decelerates the wind is speculative at present, but could be linked to the high Eddington ratios of the galaxies. Extra orientation effects (near pole-on views), considered previously to explain the correlation of [O III] blueshift with line width of blue outliers, would also explain the strong ionization stratification we detect.

5. Two blue outliers have independent BH mass/stellar velocity dispersion measurements, and these place them on or close to the $M_{\rm BH}$-$\sigma$ relation of nonactive galaxies. This, together with the fact that the width of broad H$\beta$ does not correlate with [O III] outflow velocity, indicates that if blue outliers are indeed seen more face-on, this fact does not reflect strongly in their H$\beta$ widths, implying that their BLR geometry is closer to spherical than to planar.

6. Most remarkable among the blue outliers is the galaxy RX J01354−0043. Unlike other NLS1 galaxies, its radio emission is extended and possibly double, its optical Balmer lines appear to be double-peaked, and its optical spectrum shows strong absorption lines from the host galaxy. The link between blue outliers in NLS1 galaxies and in (compact) radio galaxies needs further exploration.

D. X. acknowledges the support of the Chinese National Science Foundation (NSFC) under grant NSFC-10503005, and the support of MPG/MPE. H. Z. acknowledges support from the Alexander von Humboldt Foundation, from NSFC (grant NSF-10533050), and from program 973 (2007CB815405). L. B. acknowledges support from CONACyT grant J-50296. We thank our referee for his/her comments and suggestions, and the members of MPE's new Physics of Galactic Nuclei group and J. Sulentic, D. Proga, and D. Merritt for discussions. This research has made use of the SDSS database, and of the NASA/IPAC Extragalactic Database (NED), which is operated by the Jet Propulsion Laboratory, California Institute of Technology, under contract with the National Aeronautics and Space Administration. Funding for the SDSS and SDSS II has been provided by the Alfred P. Sloan Foundation, the Participating Institutions, the National Science Foundation, the US Department of Energy, the National Aeronautics and Space Administration, the Japanese Monbukagakusho, the Max Planck Society, and the Higher Education Funding Council for England. The SDSS is managed by the Astrophysical Research Consortium for the Participating Institutions. The Participating Institutions are the American Museum of Natural History, Astrophysical Institute Potsdam, University of Basel, University of Cambridge, Case Western Reserve University, University of Chicago, Drexel University, Fermilab, the Institute for Advanced Study, the Japan Participation Group, Johns Hopkins University, the Joint Institute for Nuclear

Astrophysics, the Kavli Institute for Particle Astrophysics and Cosmology, the Korean Scientist Group, the Chinese Academy of Sciences (LAMOST), Los Alamos National Laboratory, the Max Planck Institute for Astronomy (MPIA), the Max Planck Institute for Astrophysics (MPA), New Mexico State University, Ohio State University, University of Pittsburgh, University of Portsmouth, Princeton University, the United States Naval Observatory, and the University of Washington.

## APPENDIX

## NOTES ON INDIVIDUAL OBJECTS

A few sources are included in the SDSS-NLS1 samples of Williams et al. (2002) and Anderson et al. (2003). The high [O III] blueshifts of SDSS J115533.50+010730.4 and RX J01354−0043 were reported by Bian et al. (2005). Boroson (2005) measured [O III] blueshifts of NGC 450-86, RX J01354−0043, PG 1244+026, and SDSS 17184+5734. Here we provide a short summary of the multi-wavelength properties of the blue outliers collected from the literature, and give some comments based on our optical spectral analysis. Galaxies are listed in order of decreasing [O III] blueshift.

*SBS 0919+515*.—This AGN is a known X-ray source, first detected with the *Einstein Observatory* (Chanan et al. 1981), mostly studied in the X-ray regime (e.g., Boller et al. 1996; Vaughan et al. 2001), and optically identified as a NLS1 galaxy by Stephens (1989). It shows the highest [O III] blueshift of our sample ($v_{[\mathrm{O\,III}]} = 430$ km s$^{-1}$).

*SDSS J115533.50+010730.4*.—This AGN was detected in X-rays during the *ROSAT* All-Sky Survey (Voges et al. 1999) and was first classified as a NLS1 galaxy by Williams et al. (2002). It has the second-highest [O III] velocity shift of our sample ($v_{[\mathrm{O\,III}]} = 330$ km s$^{-1}$), has highly blueshifted [Ne V], and has faint coronal line emission of [Fe X] with a blueshift corresponding to $v_{[\mathrm{Fe\,X}]} \approx 1000$ km s$^{-1}$, among the highest blueshifts reported for coronal lines to date.

*RX J01354−0043 (SDSS J013521.68−004402.2)*.—This AGN was detected in the X-ray and radio bands (Brinkmann et al. 2000; Wadadekar 2004) and was optically identified as a NLS1 galaxy by Williams et al. (2002). It is remarkable in several respects. We find that its optical spectrum appears to be dominated by the host galaxy. Strong absorption lines from higher order Balmer lines, Ca H and K and NaID, are detected (Fig. 5). The optical AGN continuum emission is either intrinsically weak, or absorbed (which would require a peculiar geometry of the absorber, given that the broad Balmer lines are present). RX J01354−0043 is detected with *GALEX*[6] and displays red UV colors. Its (narrow) Balmer lines appear double-peaked, with a separation of ∼580 km s$^{-1}$, or else are affected by residual, exceptionally strong and redshifted host galaxy features, which is very unlikely, given the strength of H$\alpha$. The line decomposition

[6] See http://galex.stsci.edu/GR2/.

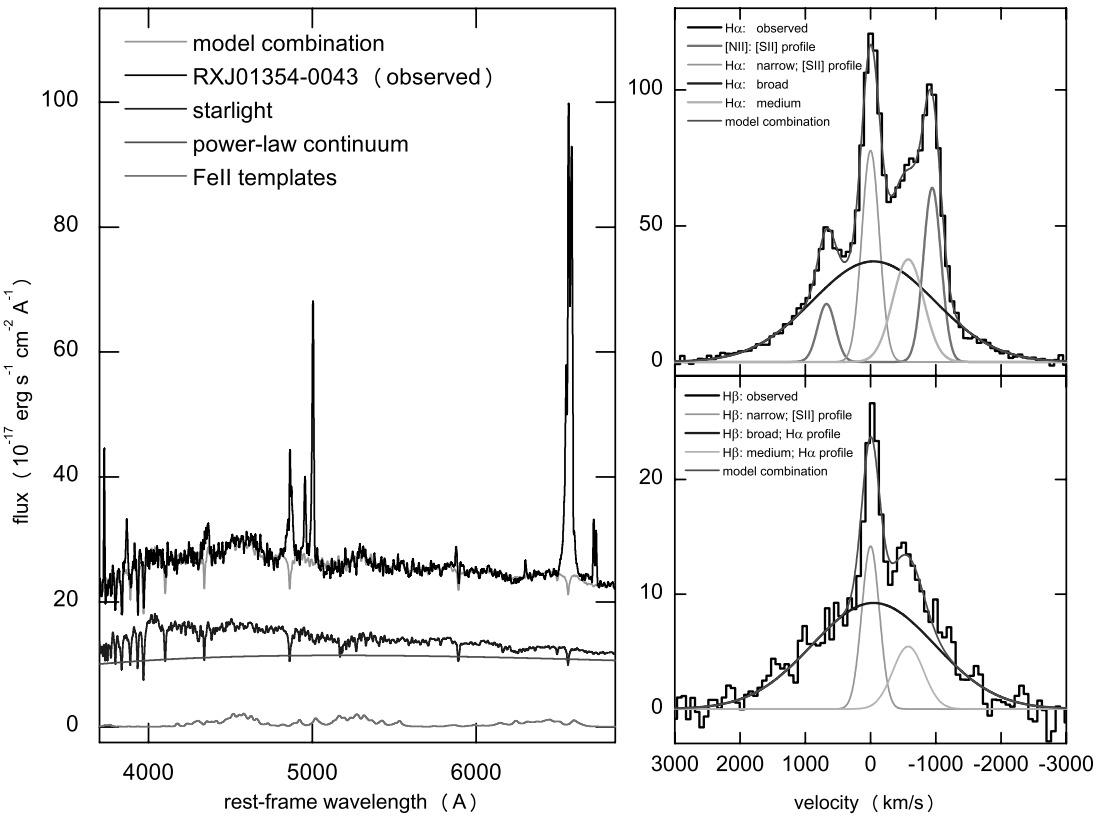


FIG. 5.—*Left*: SDSS spectrum of RX J0135−0043, and component decomposition into Fe II complexes, a reddened AGN power-law continuum, and host galaxy contribution as labeled in the figure. Strong absorption lines from the host galaxy are visible. *Right*: Zoom onto the H$\alpha$ and H$\beta$ lines, showing the presence of two narrow cores of each Balmer line (*lower gray lines*; note that in this paper, we use positive velocities to indicated blueshifts, and negative values for redshifts), and a broad base (*smooth black lines*). [*See the electronic edition of the Journal for a color version of this figure*.]

shown in Figure 5 assumes the same widths of the narrow core of H$\beta$ and of the two [N II] lines, fixed to the width of [S II], and further assumes a fixed [N II] line ratio. The remaining profile was modeled with two Gaussians of free parameters and can be well fit with a broad component plus a second, redshifted relatively narrow component. RX J01354−0043 has a *FIRST* detection with a radio flux of 2 mJy and there is evidence for extended radio emission (White et al. 1997),[7] corresponding to a scale of ∼10 kpc. This is remarkable because few if any NLS1 galaxies are known to have widely extended radio emission (Ulvestad et al. 1995; Komossa et al. 2006; Yuan et al. 2008). Inspecting the *FIRST* image cut-out, the source appears to be double. Among the emission lines, only the Balmer lines appear double-peaked. RX J01354−0043 is the first blue outlier to show this phenomenon. Explanations include jet-cloud interaction, a bipolar outflow, or, speculatively, superposed strong Balmer absorption (which is rarely seen because the required level population is not easy to achieve; Hall 2007; H. Lu et al., in preparation). We have used the stellar absorption lines from the host galaxy for a measurement of $\sigma_*$. We obtain $\sigma_* = 82$ km s$^{-1}$, which is in good agreement with the [S II]–based measurement, $\sigma_{[S\,II]} = 106$ km s$^{-1}$, and locates RX J01354−0043 (almost perfectly) on the $M_{BH}$-$\sigma_*$ relation of nonactive galaxies (Fig. 1).

*NGC 450-86*.—Identified as a NLS1 galaxy by Williams et al. (2002) and detected in X-rays during the *ROSAT* All-Sky Survey (Voges et al. 1999).

*SDSS J032606.75+011429.9*.—A basically unknown galaxy, with an optical NLS1 spectrum (Williams et al. 2002). No radio or X-ray detection was reported.

*IRAS 11598−0112*.—This galaxy is ultraluminous in the infrared (Murphy et al. 1996; Kim & Sanders 1998) with a single nucleus and prominent tidal tails (Veilleux et al. 2002). Its optical spectrum is that of a NLS1 galaxy (Moran et al. 1996). It is almost radio-loud with a 1.4 GHz radio index $R \approx 5$ (Komossa et al. 2006) and was first detected in X-rays with *ROSAT* (Voges et al. 1999). The Fe II emission in its optical spectrum is not well described by our Fe II template. In particular, the "red" and "blue" complexes of Fe II do not match each other well, and the source redshift appears to differ from that of Fe II. Strong emission of unknown nature remains blueward of [O III]. Formally, we can describe it with an extra [O III] component, broad [FWHM([O III]) = 1800 km s$^{-1}$] and highly blueshifted ($v = 1300$ km s$^{-1}$). If real, it could represent an extreme blue wing, or could imply the presence of an extra starburst/shock-driven component. The structure needs to be confirmed by independent spectroscopy.

*SDSS J171828.99+573422.3*.—Detected with *ROSAT* (Brinkmann et al. 1999), and optically identified as a NLS1 galaxy by Williams et al. (2002).

*PG 1244+026*.—This AGN (Green et al. 1986) is a well-known X-ray, UV, infrared, and radio source (e.g., Elvis et al. 1986; Kellerman et al. 1989; Sanders et al. 1989; Fiore et al. 1998; Ballantyne et al. 2001; Jimènez-Bailòn et al. 2005) with an optical NLS1 spectrum (Miller et al. 1992; Veron-Cetty et al. 2001). It is radio-quiet with a 5 GHz radio index of $R = 0.5$ (Kellerman et al. 1989). Hayashida (2000) and Czerny et al. (2001) determined its black hole mass based on X-ray variability (the power density spectrum). Czerny et al. (2001) report $\log M_{BH} = 5.9$, which is consistent with our value of $\log M_{BH} = 6.2$ from applying the relation of Kaspi et al. (2005). We detect in its optical spectrum [Fe X] emission with an outflow velocity of 640 km s$^{-1}$.

*RX J09132+3658*.—Detected in X-rays with *ROSAT* (Voges et al. 1999; Brinkmann et al. 2000) and in the radio band during the *FIRST* survey (White et al. 1997), and identified as a NLS1 galaxy by Xu et al. (1999).

[7] The most recent catalog update is at http://cdsarc.u-strasbg.fr/viz-bin/Cat?VIII/71.

## REFERENCES


Abazajian, K., et al. 2005, AJ, 129, 1755
Anderson, S. F., et al. 2003, AJ, 126, 2209
Aoki, K., Kawaguchi, T., & Ohta, K. 2005, ApJ, 618, 601
Ballantyne, D. R., Iwasawa, K., & Fabian, A. C. 2001, MNRAS, 323, 506
Barth, A. J., Greene, J. E., & Ho, L. C. 2005, ApJ, 619, L151
Bennert, N., Jungwiert, B., Komossa, S., Haas, M., & Chini, R. 2006, A&A, 456, 953
Bian, W., Yuan, Q., & Zhao, Y. 2005, MNRAS, 364, 187
Bian, W., & Zhao, Y. 2004, MNRAS, 347, 607
Binette, L. 1998, MNRAS, 294, L47
Binette, L., Wilson, A. S., Raga, A., & Storchi-Bergmann, T. 1997, A&A, 327, 909
Blandford, R., & Königl, A. 1979, Astrophys. Lett., 20, 15
Boller, T., Brandt, W. N., & Fink, H. 1996, A&A, 305, 53
Bonning, E. W., Shields, G. A., & Salviander, S. 2007, ApJ, 666, L13
Boroson, T. A. 2002, ApJ, 565, 78
———. 2003, ApJ, 585, 647
———. 2005, ApJ, 130, 381
Botte, V., Ciroi, S., Di Mille, F., Rafanelli, P., & Romano, A. 2005, MNRAS, 356, 789
Botte, V., Ciroi, S., Rafanelli, P., & Di Mille, F. 2004, AJ, 127, 3168
Brinkmann, W., et al. 1999, A&AS, 134, 221
———. 2000, A&A, 356, 445
Campanelli, M., Lousto, C. O., Zlochower, Y., & Merritt, D. 2007, Phys. Rev. Lett., 98, 1102
Cecil, G., et al. 2002, ApJ, 568, 627
Chanan, G. A., Margon, B., & Downes, R. A. 1981, ApJ, 243, L5
Chelouche, D., & Netzer, H. 2005, ApJ, 625, 95
Churazov, E., Brüggen, M., Kaiser, C. R., Böhringer, H., & Forman, W. 2001, ApJ, 554, 261
Colbert, E. J. M., et al. 1996, ApJS, 105, 75
Crenshaw, D. M., & Kraemer, S. B. 2007, ApJ, 659, 250
Czerny, B., Nikolajuk, M., Piasecki, M., & Kuraszkiewicz, J. 2001, MNRAS, 325, 865
Das, V., Crenshaw, D. M., & Kraemer, S. B. 2007, ApJ, 656, 699
Das, V., et al. 2005, AJ, 130, 945
de Robertis, M., & Osterbrock, D. E. 1984, ApJ, 286, 171
di Matteo, T., Springel, V., & Hernquist, L. 2005, Nature, 433, 604
Dopita, M., Groves, B. A., Sutherland, R. S., Binette, L., & Cecil, G. 2002, ApJ, 572, 753
Elvis, M. 2000, ApJ, 545, 63
———. 2006, Mem. Soc. Astron. Italiana, 77, 573
Elvis, M., et al. 1986, ApJ, 310, 291
Erkens, U., Apenzeller, I., & Wagner, S. 1997, A&A, 323, 707
Everett, J. E. 2007, Ap&SS, 311, 269
Everett, J. E., & Murray, N. 2007, ApJ, 656, 93
Fabian, A. 1999, MNRAS, 308, L39
Fabian, A., Celotti, A., & Erlund, M. C. 2006, MNRAS, 373, L16
Falcke, H., Wilson, A. S., & Simpson, C. 1998, ApJ, 502, 199
Fedorenko, V. N., Paltani, S., & Zentsova, A. S. 1996, A&A, 314, 368
Ferrarese, L., & Ford, H. 2005, Space Sci. Rev., 116, 523
Ferrarese, L., & Merritt, D. 2000, ApJ, 539, L9
Fiore, F., et al. 1998, MNRAS, 298, 103
Gallimore, J. F., Axon, D. J., O'Dea, C., Baum, S. A., & Pedlar, A. 2006, AJ, 132, 546
Gaskell, C. M. 1982, ApJ, 263, 79
Gebhardt, K., et al. 2000, ApJ, 539, L13
Grandi, S. A. 1977, ApJ, 215, 446
Green, R. F., Schmidt, M., & Liebert, J. 1986, ApJS, 61, 305
Greene, J. E., & Ho, L. C. 2005, ApJ, 627, 721
Grupe, D. 2004, AJ, 127, 1799
Grupe, D., & Mathur, S. 2004, ApJ, 606, L41
Gupta, N., Srianan, R., & Saiki, D. J. 2005, MNRAS, 361, 451
Hall, P. 2007, AJ, 133, 1271

Hayashida, K. 2000, NewA Rev., 44, 419
Heckman, T. M., Miley, G. K., van Breugel, W. J. M., & Butcher, H. R. 1981, ApJ, 247, 403
Holt, J., Tadhunter, C. N., & Morganti, R. 2003, MNRAS, 342, 227
Holt, J., et al. 2006, MNRAS, 370, 1633
Jimènez-Bailòn, E., et al. 2005, A&A, 435, 449
Kaspi, S., et al. 2000, ApJ, 533, 631
———. 2005, ApJ, 629, 61
Kellermann, K. I., Sramek, R., Schmidt, M., Shaffer, D. B., & Green, R. 1989, AJ, 98, 1195
Kim, D.-C., & Sanders, D. B. 1998, ApJS, 119, 41
Komossa, S. 2008, RevMexAA, in press (arXiv:0710.3326v1)
Komossa, S., & Schulz, H. 1997, A&A, 323, 31
Komossa, S., & Xu, D. 2007, ApJ, 667, L33 (KX07)
Komossa, S., et al. 2006, AJ, 132, 531
Königl, A. 2006, Mem. Soc. Astron. Italiana, 77, 598
Krause, M. 2007, NewA Rev., 51, 174
Kriss, G. A. 1994, in ASP Conf. Ser. 61, Astronomical Data Analysis Software and Systems III, ed. D. R. Crabtree, R. J. Hanisch, & J. Barnes (San Francisco: ASP), 437
Krolik, J. H., & Vrtilek, J. M. 1984, ApJ, 279, 521
Krongold, Y., Dultzin-Hacyan, D., & Marziani, P. 2001, AJ, 121, 702
Krongold, Y., et al. 2007, ApJ, 659, 1022
Laor, A., Jannuzi, B. T., Green, R. F., & Boroson, T. A. 1997, ApJ, 489, 656
Marziani, P., Zamanov, R. K., Sulentic, J. W., & Calvani, M. 2003, MNRAS, 345, 1133
Mathews, W. G., & Veilleux, S. 1989, ApJ, 336, 93
Mathur, S., & Grupe, D. 2005a, ApJ, 633, 688
———. 2005b, A&A, 432, 463
Mathur, S., Kuraszkiewicz, J., & Czerny, B. 2001, NewA, 6, 321
Miller, P., Rawlings, S., Saunders, R., & Eales, S. 1992, MNRAS, 254, 93
Moll, R., et al. 2007, A&A, 463, 513
Moran, E. C., Halpern, J. P., & Helfand, D. J. 1996, ApJS, 106, 341
Morganti, R., Holt, J., Saripalli, L., Oosterloo, T. A., & Tadhunter, C. N. 2007, A&A, 476, 735
Morganti, R., Tadhunter, C. N., & Oosterloo, T. A. 2005, A&A, 444, L9
Murphy, T. W., et al. 1996, AJ, 111, 1025
Nelson, C. H. 2000, ApJ, 544, L91
Nelson, C. H., & Whittle, M. 1996, ApJ, 465, 96
Netzer, H., & Trakhtenbrot, B. 2007, ApJ, 654, 754
Osterbrock, D. E. 1991, Rep. Prog. Phys., 54, 579
Osterbrock, D. E., & Pogge, R. 1985, ApJ, 297, 166
Ostriker, E. C., Lee, C.-F., Stone, J. M., & Mundy, L. G. 2001, ApJ, 557, 443
Penston, M. S., Fosbury, R. A. E., Boksenberg, A., Ward, M. J., & Wilson, A. S. 1984, MNRAS, 208, 347
Phillips, M. M. 1976, ApJ, 208, 37
Pretorius, F. 2007, preprint (arXiv:0710.1338)
Proga, D. 2007, in ASP Conf. Ser. 373, The Central Engine of Active Galactic Nuclei, ed. L. C. Ho & J.-M. Wang (San Francisco: ASP), 267
Proga, D., Ostriker, J. P., & Kurosawa, R. 2008, ApJ, 676, 101
Rice, M., et al. 2006, ApJ, 636, 654
Riffel, R. A., Storchi-Bergmann, T., Winge, C., & Barbosa, F. K. B. 2006, MNRAS, 373, 2
Rodriguez-Ardila, A., Prieto, M. A., Viegas, S., & Gruenwald, R. 2006, ApJ, 653, 1098
Rodriguez Hidalgo, P., Hamann, F., Nestor, D., & Shields, J. 2007, in ASP Conf. Ser. 373, The Central Engine of Active Galactic Nuclei, ed. L. C. Ho & J.-M. Wang (San Francisco: ASP), 287
Rupke, D. S., Veilleux, S., & Sanders, D. B. 2005, ApJ, 632, 751
Ryan, C. J., de Robertis, M. M., Virani, S., Laor, A., & Dawson, P. C. 2007, ApJ, 654, 799
Salviander, S., Shields, G. A., Gebhardt, K., & Bonning, E. W. 2007, ApJ, 662, 131
Sanders, D. B., Phinney, E. S., Neugebauer, G., Soifer, B. T., & Mathews, K. 1989, ApJ, 347, 29
Saxton, C. J., Bicknell, G. V., Sutherland, R. S., & Midgley, S. 2005, MNRAS, 359, 781
Scannapieco, E., Silk, J., & Bouwens, R. 2005, ApJ, 635, L13
Schiano, A. V. R. 1986, ApJ, 302, 81
Schiano, A. V. R., Christiansen, W. A., & Knerr, J. M. 1995, ApJ, 439, 237
Schinnerer, E., Eckart, A., & Tacconi, L. J. 1998, ApJ, 500, 147
Schulz, H. 1990, AJ, 99, 1442
Shields, G. A., et al. 2003, ApJ, 583, 124
Silk, J., & Rees, M. 1998, A&A, 331, L1
Smith, S. J. 1993, ApJ, 411, 570
Springel, V., Di Matteo, T., & Hernquist, L. 2005, ApJ, 620, L79
Stephens, S. 1989, AJ, 97, 10
Stockton, A., Canalizo, G., Fu, H., & Keel, W. 2007, ApJ, 659, 195
Stojimirović, I., Narayan, G., Snell, R. L., & Bally, J. 2006, ApJ, 649, 280
Sulentic, J., Bachev, R., Marziani, P., Negrete, C. A., & Dultzin, D. 2007, ApJ, 666, 757
Tadhunter, C., Wills, K., Morganti, R., Oosterloo, T., & Dickson, R. 2001, MNRAS, 327, 227
Terlevich, E., Diaz, A. I., & Terlevich, R. 1990, MNRAS, 242, 271
Tremaine, S., et al. 2002, ApJ, 574, 740
Ulvestad, J. S., Antonucci, R. R. J., & Goodrich, R. W. 1995, AJ, 109, 81
Vaughan, S., Edelson, R., Warwick, R. S., Malkan, M. A., & Goad, M. R. 2001, MNRAS, 327, 673
Veilleux, S. 1991, ApJ, 369, 331
Veilleux, S., Cecil, G., & Bland-Hawthorn, J. 2005, ARA&A, 43, 769
Veilleux, S., Kim, D.-C., & Sanders, D. B. 2002, ApJS, 143, 315
Véron, M. P. 1981, A&A, 100, 12
Véron-Cetty, M. P., Joly, M., & Véron, P. 2004, A&A, 417, 515
Véron-Cetty, M. P., & Véron, P. 2003, A&A, 412, 399
Véron-Cetty, M. P., Véron, P., & Goncalves, A. C. 2001, A&A, 372, 730
Voges, W., et al. 1999, A&A, 349, 389
Wadadekar, Y. 2004, A&A, 416, 35
Wandel, A. 2002, ApJ, 565, 762
Wang, T., & Lu Y. 2001, A&A, 377, 52
Watson, L., Mathur, S., & Grupe, D. 2007, AJ, 133, 2435
White, R. L., Becker, R. H., Helfand, D. J., & Gregg, M. D. 1997, ApJ, 475, 479
Whittle, M. 1992, ApJ, 387, 109
Williams, R. J., Pogge, R. W., & Mathur, S. 2002, AJ, 124, 3042
Wyithe, J. S. B., & Loeb. A. 2003, ApJ, 595, 614
Xu, D., Komossa, S., Zhou, H., Wang, T., & Wei, J. 2007, ApJ, 670, 60
Xu, D., Wei, J. Y., & Hu, J. Y. 1999, ApJ, 517, 622
Young, S., Axon, D. J., Robinson, A., Hough, J. H., & Smith, J. E. 2007, Nature, 450, 74
Yuan, W., et al. 2008, ApJ, submitted
Zamanov, R., et al. 2002, ApJ, 576, L9
Zhou, H.-Y., et al. 2006, ApJS, 166, 128